bioresources.com

Superabsorbent Sponge and Membrane Prepared by Polyelectrolyte Complexation of Carboxymethyl Cellulose/Hydroxyethyl Cellulose-Al^{3+}

Yang Liu, Yu Chen,* Ying Zhao, Zongrui Tong, and Shuseng Chen

A novel carboxymethyl cellulose/ hydroxyethyl cellulose-Al^{3+} (CMC/HEC-Al^{3+}) hydrogel was prepared through electrostatic complexing between the anionic polyelectrolyte CMC and cationic cross-linking agent Al^{3+}. The structure and properties of the hydrogel were characterized using FTIR, TGA, and SEM. The viscoelasticities of the swollen hydrogel were measured using the rheology test. The results indicated that a porous network structure was formed in the hydrogel. The content of CMC, HEC, and Al^{3+} can significantly affect its structure and characteristics. A sponge and membrane were prepared from the CMC/HEC-Al^{3+} hydrogel by freeze-drying and oven drying, respectively. Their swelling behaviors were investigated in water and saline solutions, and quantified with a swelling kinetic simulation. The results indicated that electrostatic effects, physical entanglement, and intra- and intermolecular hydrogen bonds contributed to the cross-linking network structure, with the electrostatic effect acting as the dominant force. In all, both superabsorbent sponge and membrane prepared from CMC/HEC-Al^{3+} hydrogel showed excellent swelling behavior and could be used in dressing wounds.

*Contact information: School of Material Science and Engineering, Beijing Institute of Technology, Beijing 100081, P. R. China; *Corresponding author: cylsy@163.com*

INTRODUCTION

A hydrogel is a highly absorbent, three-dimensional polymer network (Chang *et al.* 2010; Laçin 2014). It can absorb large volumes of liquid solution and swell significantly. The swelling capability of a hydrogel depends on the skeleton and crosslinking density of its network (Chen *et al.* 2009; Coviello *et al.* 2010).

Carbohydrate polymers, such as alginate, starch, cellulose, and chitosan, are good skeleton candidates for hydrogels due to their excellent biocompatibility, biodegradability, and bioactivity (Liu *et al.* 2009; Coviello *et al.* 2010). They have been widely used in the preparation of hydrogels for biomedical, tissue engineering, drug delivery, and pharmaceutical purposes (Schrecker and Gostomski 2005; Tang *et al.* 2014).

The anionic polyelectrolyte carboxymethyl cellulose (CMC) is an important derivative of cellulose with good water solubility resulting from the –CH$_2$COOH groups in its skeleton (Barbucci *et al.* 2000). It has attracted considerable attention due to its unique properties such as high viscosity, transparency, hydrophilicity, non-toxicity, biocompatibility, biodegradability, and good film forming ability (Yang and Zhu 2007; Ibrahim *et al.* 2014).

Hydrogels prepared through the crosslinking of CMC are highly absorbent with excellent physical properties and dynamic viscoelasticities (Nerurkar *et al.* 2010). However, CMC itself tends to form intramolecular rather than intermolecular crosslinks in a solution. Therefore, hydroxyethylcellulose (HEC) is usually introduced to avoid the formation of intramolecular crosslinks (Seki *et al*. 2014). The hydrogels prepared from carboxymethyl cellulose/hydroxyethyl cellulose (CMC/HEC) may potentially be used in many fields such as food additives, cosmetics, wound dressing, tissue engineering, and cell culture substrate (Saha *et al.* 2011; Gao *et al.* 2014; Kono 2014). Most CMC hydrogels are prepared through chemical cross-linking reactions. The cross-linking network prepared by chemical reaction is usually robust, exhibits good mechanical properties, and excellent water absorption properties. However, the toxic and carcinogenic residuals of the cross-linking agent, and the byproducts in the hydrogel, limit its application in drug delivery and other biological processes. In addition, the network structure prepared through the chemical cross-linking is non-uniform due to the rapid chemical reaction, which affects its extension in the absorbent solution.

Electrostatic complexing can be used as a novel method to construct 3-D polymer network structures in hydrogels. For example, Hossein *et al*. (2010) developed hydrogels using the cross-linking of poly(acrylic acid) and poly(2-hydroxyethyl methacrylate), with calcium and aluminum ions serving as the cross-linking agents. The hydrogels showed no significant cytotoxicity and stimulatory effects (Omidian *et al*. 2010; Hubbe *et al*. 2013).

Aluminum sulfate, with its cationic species in the effective forms of Al^{3+}, $Al(OH)^{2+}$, and oligomeric species in aqueous solution when pH < 5, provides multivalent positive charges and abundant sites for cross-linking with anionic groups. Aluminum sulfate has been widely used as a cross-linking agent in the preparation of biomaterials and exhibits excellent performance and low toxicity. It is an excellent candidate for the electrostatic complexing with the polymers containing $–COO^-$ groups to form hydrogel structures (Bi *et al*. 2004).

In the present study, a novel electrostatic complexing method is proposed for the preparation of CMC/HEC hydrogels with aluminum ions as a cross-linker (Sannino and Nicolais 2005; Seki *et al*. 2014). The structure of the prepared hydrogels was characterized and the effects of the preparation condition on its properties was investigated. Due to its unique properties, the CMC/HEC-based hydrogel is a potential candidate of wound dressing.

EXPERIMENTAL

Materials

USP grade carboxymethyl cellulose (CMC) with a viscosity of 300 to 800 mPa·s (1% aqueous solution, 25 °C) and hydroxyethyl cellulose (HEC) with a viscosity of 80 to 125 mPa·s (1% aqueous solution, 25 °C) were obtained from Aladdin Industrial Co, Ltd. (Hangzhou, China).

Analytical grade $Al_2(SO_4)_3·18H_2O$, NaCl, and C_2H_5OH were purchased from Beijing Chemical Works (Beijing, China). All reagents were used as obtained without further purification.

Methods

Preparation of CMC/HEC-Al^{3+} hydrogel

A series of CMC/HEC-Al^{3+} polyelectrolyte complexation hydrogels were prepared. The term Al^{3+}, when used in the discussion that follows, will be intended to include other cationic species, depending on the pH and other factors. In a typical procedure, a certain amount of CMC and HEC were dissolved in distilled water under 300 rpm of stirring which could make the segment of CMC more stretch, resulting in a solution with 3% CMC and 1% HEC. The solution (pH=7.8) was heated in a water bath at 25 °C for 40 min. Then 10 mL of aluminum sulfate solution (pH=3.4) at a certain concentration was added drop by drop into the CMC/HEC solution, and the mixture was stirred for 20 min. The resultant hydrogel was poured into two petri dishes and freeze-dried and force air dried, respectively, to a constant weight to make superabsorbent sponge and membrane materials.

Swelling kinetics of CMC/ HEC-Al^{3+} hydrogel

The swelling behavior of CMC/HEC-Al^{3+} dried hydrogel was investigated using the tea-bag method (Japan Industrial Standard, JIS K7223) (Kono and Fujita 2012). A 10 × 10 mm sample was put into a tea bag and immersed in distilled water or saline water at 25 °C (Chen *et al.* 2010). The tea bag with the sample was removed from the aqueous solution at regular time intervals and weighed after the excess solution was removed. The percentage of water uptake capacity at time *t* was calculated with the following equation (Eq. 1):

$$Q = \frac{Wt - Wd}{Wd} \times 100$$

(1)

where *Q* is the water absorbency (%) at time *t*, *Wt* is the weight of the swollen hydrogel at time *t*, and *Wd* is the initial weight of the sample. Three parallel experiments were conducted and the average values were calculated.

Fourier transform infrared (FT-IR) spectroscopy

A 1 mg sample was ground, mixed well with 100 mg KBr power, and compressed into a transparent disk. The FTIR spectra of the CMC/HEC-Al^{3+} dried hydrogels and raw material were recorded on a Fourier transform infrared spectrometer (Nicolet 380, Thermo Electron Co., USA) in the range 4000 to 500 cm^{-1} using an average of 16 scans with a resolution of 1 cm^{-1}.

Morphological analysis

The hydrogel products were lyophilized, fixed on a metal stub with conductive tape, sputter-coated with a gold layer, and examined with a scanning electron microscope (SEM, Hitachi S–4800, Japan).

Thermogravimetric analyses

Thermogravimetric analyses were conducted on a thermal gravimetric analyzer (DTG-60, Shimadzu, Japan). The sample was heated from 30 to 500 °C at 10 °C/min under a nitrogen flow of 50 mL/min.

Dynamic rheology analyses

The prepared cellulose derivative hydrogel was degassed and analyzed on a dynamic viscoelastic rheometer (Anton Paar, MCR 301, Austria) at a constant temperature in a sweeping frequency range from 0.01 to 100 rad/s.

RESULTS AND DISCUSSION

Fourier Transform Infrared Spectroscopy Analyses

Figure 1 shows the FT-IR spectra of CMC and CMC/HEC-Al^{3+} dried hydrogel. The asymmetric stretching vibration and symmetrical stretching of the –COO^- group in CMC showed absorption peaks at 1635 cm^{-1} and 1424 cm^{-1}, respectively. The asymmetric stretching vibration peak of the –COO^- group in CMC/HEC-Al^{3+} hydrogel shifted to 1610 cm^{-1} and its symmetrical stretching was remained at 1424 cm^{-1}.
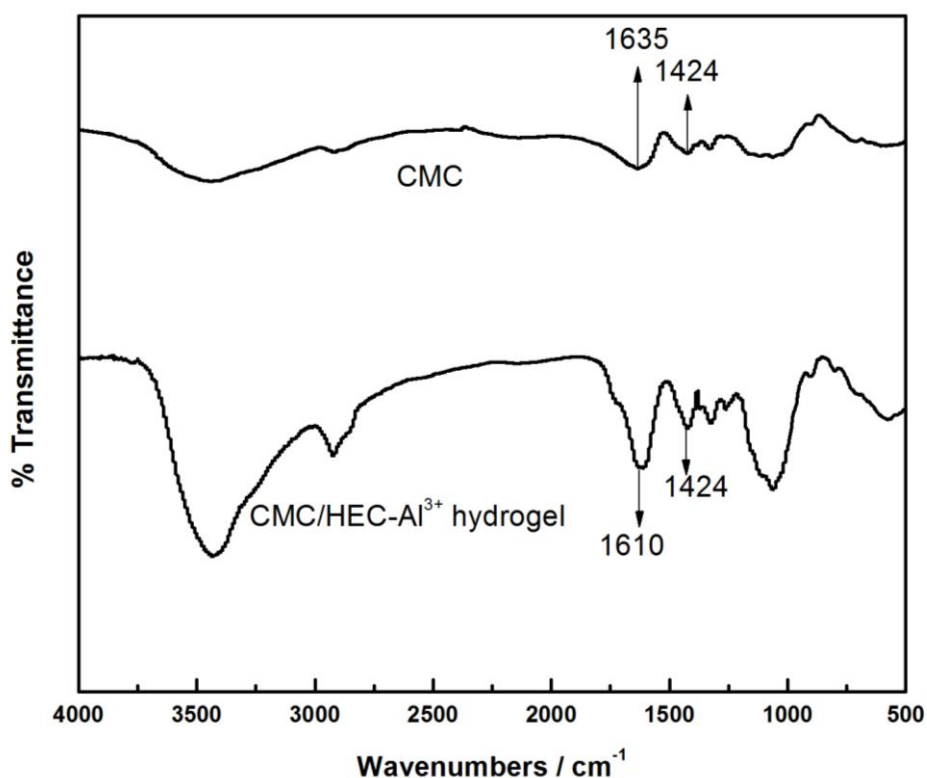
Fig. 1. FT-IR spectra of CMC and CMC/HEC-Al^{3+} dried hydrogel

It has been reported that the shift in frequency (Δv), *e.g.* v_a-v_s, toward –COO^- of a coordination compound compared to that of the single ligand can be used to characterize the coordination band between the ligand and its ion coordination center (Nakamoto 2008). A higher Δv value of coordination compound indicates the occurrence of unidentate ligand reaction, and a lower Δv value indicates the occurrence of a bidentate ligand reaction. The Δv values of the CMC and CMC/HEC-Al^{3+} hydrogel were 211 cm^{-1} and 186 cm^{-1}, respectively, indicating the occurrence of bidentate ligand reactions between the aluminum ions and carboxyl groups of CMC (Fig. 2).
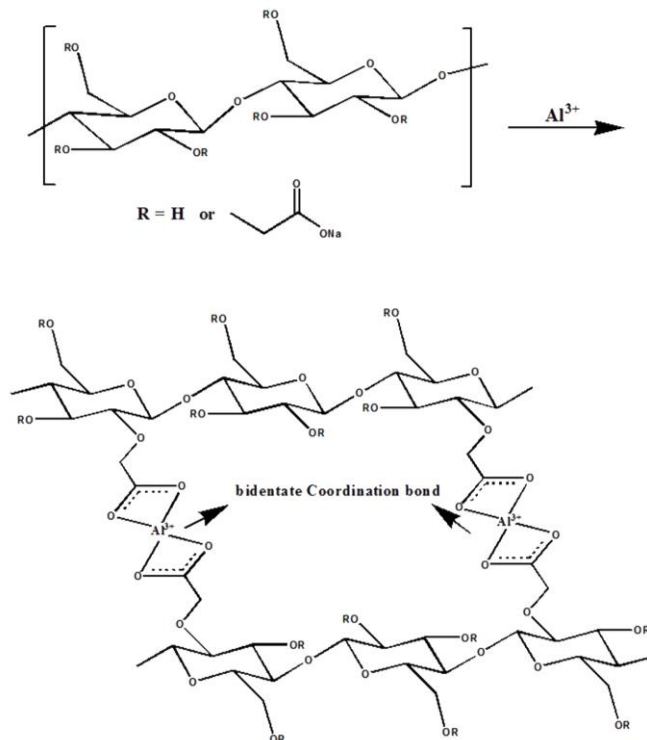
Fig. 2. Formation of the bidentate coordination ionic interactions in the CMC/HEC-Al^{3+} hydrogel

Dynamic Rheology Analyses

The storage modulus (G') and loss modulus (G'') of a hydrogel can be used to determine its gelation structure (Cai and Zhang 2006). The storage modulus G' describes the rheological behavior of a solid-like component. It is low in a solution phase, dramatically increases near the gelation point, and crosses with G'' at the gelation point. The higher G' above the gelation point indicates the formation of cross-linked hydrogel. The G' values of all samples were higher than their corresponding G'' values, indicating the formation of cross-linked networks in the CMC/HEC-Al^{3+} hydrogels (Fig. 3).
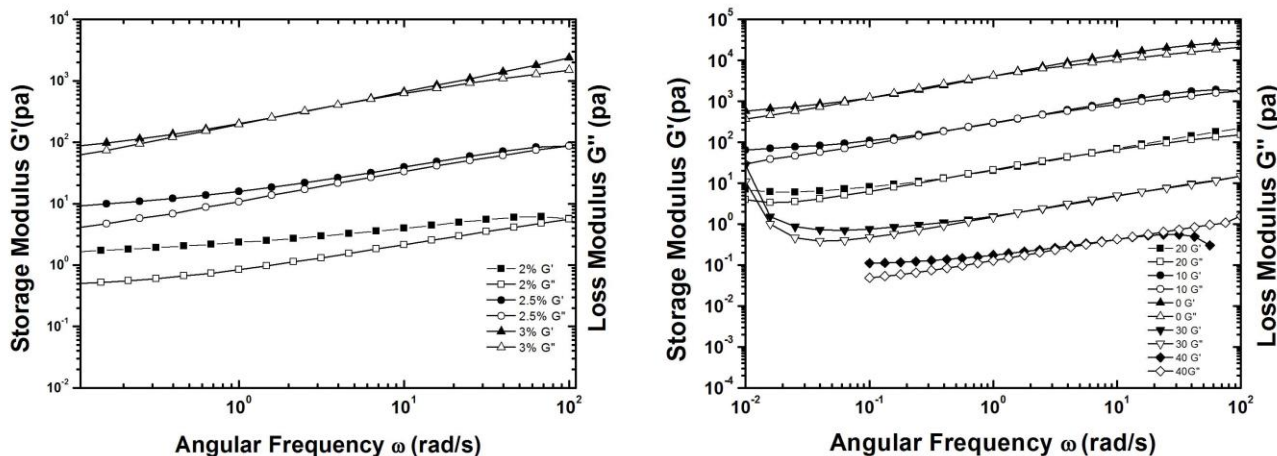
Fig. 3. Storage modulus G′, and loss modulus G″ as a function of angular frequency ω at (a) various temperatures for 3 wt% CMC/HEC-Al^{3+} hydrogel, and (b) for CMC/HEC-Al^{3+} hydrogel with different concentrations at 25 °C

The effects of temperature and CMC/HEC content on the rheological properties of CMC/HEC-Al^{3+} hydrogel were also investigated. Figure 3a shows the shear storage modulus (G') and shear loss modulus (G'') at various temperatures as the function of angular frequency (ω) of a CMC/HEC-Al^{3+} hydrogel with 3 wt% CMC. It can be seen that G' was higher than $\underline{G''}$, and both G' and G'' increased with the decrease of temperature in the whole accessible frequency range, indicating the occurrence of intra- and intermolecular cross-linkings between CMC/HEC and Al^{3+} ions in the hydrogel, and the aggregation and entanglements of the cellulose chains at lower temperatures (Weng *et al.* 2004). Therefore, cellulose chains became stiffer and had stronger interactions at low temperatures.

Figure 3b shows the G' and G'' curves as a function of angular frequency of the CMC/HEC-Al^{3+} hydrogel with different CMC/HEC contents. It is clear that G' was higher than G'' at the corresponding frequency throughout the whole range, and both were increased with increases of the CMC/HEC content in the whole accessible frequency range, suggesting that the cross-linking density of the hydrogels increased with the increase of polymer content. The entangling effects of the natural polymer became more obvious at higher CMC and HEC contents. Meanwhile, more –COOH groups were available to promote the cross-linking efficiency of cationic aluminum species.

Swelling Properties of the CMC/HEC-Al^{3+} Hydrogel

The Voigt model can be used to simulate the deformation of a viscoelastic material under constant external forces over the course of time (Chen and Tan 2006). This deformation process is known as creep in material science. The swelling process of hydrogel is similar to the creep. Therefore, the Voigt model was used to simulate the swelling kinetics of the hydrogel (Chen *et al.* 2012). The swelling process was described with the following equation (Eq. 2),

$$\varepsilon(t) = \sigma/E\{1\text{-}\exp[(t_0\text{-}t)/\tau_0]\} = \varepsilon(\infty)\{1\text{-} \exp[(t_0\text{-}t)/\tau_0]\} \tag{2}$$

where τ_0 is the relaxation time describing the resistance of polymer to water penetration, $\varepsilon(t)$ is the swelling ratio of dry hydrogels at time t, and $\varepsilon(\infty)$ is the maximum or equilibrium swelling ratio. The value of τ_0 can be obtained from the negative reciprocal of the slope of ln $[1\text{-}\varepsilon(t)/\varepsilon(\infty)]$ to the t curve.

Theoretically, the smaller τ_0 value indicates easier water penetration through the network, a faster water absorption rate, and vice versa. Therefore, it can be used to determine the water absorption rate on macro-scales. E is Young's modulus, which describes the resistance of a material to deformation in the Voigt model. The E of a hydrogel indicates the resistance of the polymer network structure to the infinite expansion of the molecular chains. The parameter k can be obtained from the slope of the linear portion of swelling kinetic curves. It is also an important index reflecting the swelling rate of a polymer.

Figure 4 shows the experimental and simulated swelling kinetic curves of the CMC/HEC-Al^{3+} hydrogels prepared under different conditions in distilled water and saline solution at 25 °C. It can be clearly seen that the simulated swelling curves constructed with the Voigt model are consistent with the experimental results. The kinetic parameters were then deduced from the kinetic model and used to compare the swelling kinetics of the hydrogels prepared under various conditions (Tables 1 and 2).
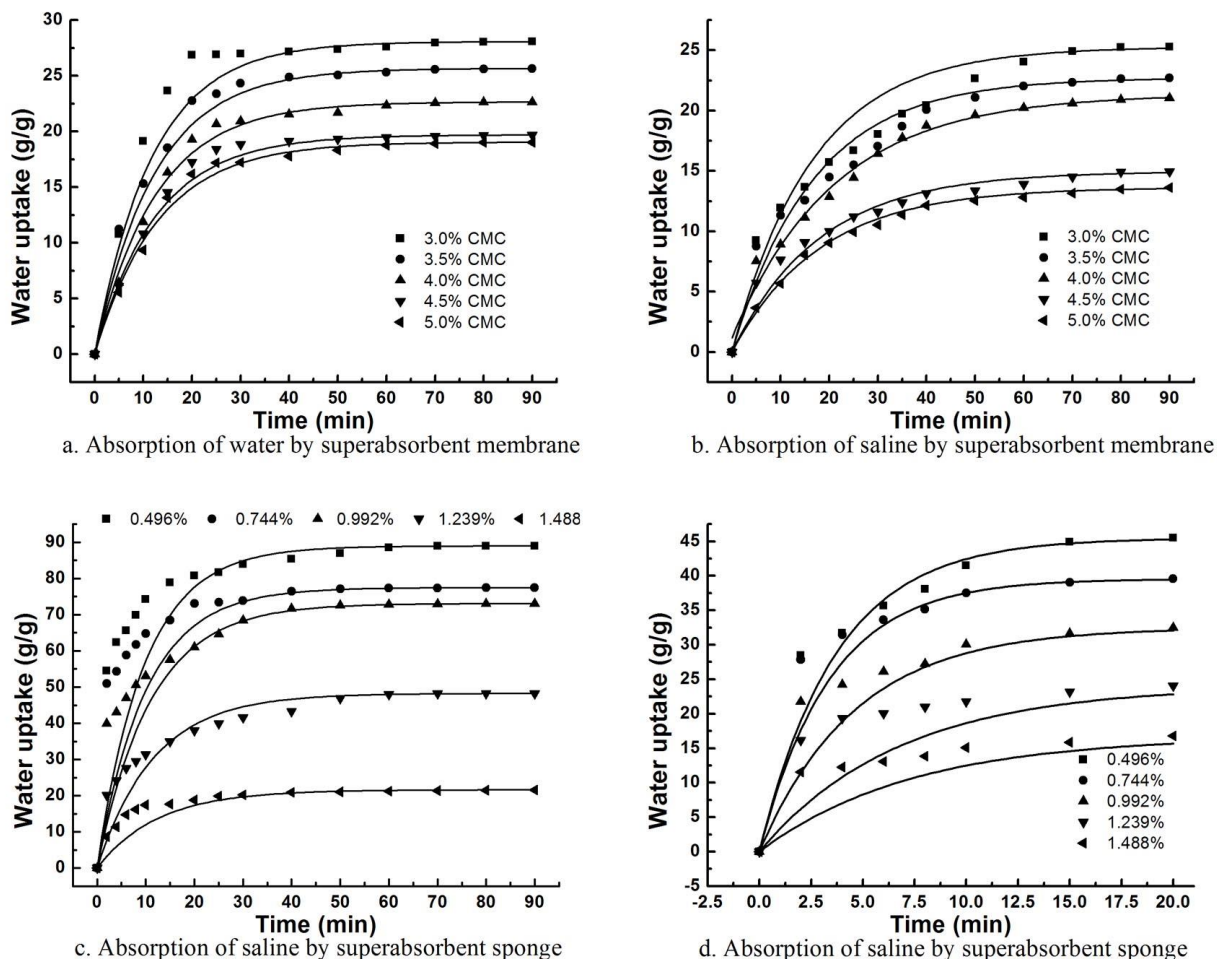
Fig. 4. Effect of the mass fraction of CMC/HEC (a, b) and cross-linker content (c, d) on the swelling property of CMC/HEC-Al^{3+} superabsorbent membrane and sponge in water and saline

Swelling rate of CMC/HEC-Al^{3+} hydrogel

The swelling ratios and water absorption rates of the superabsorbent sponge and membrane are shown in Tables 1 and 2, respectively.

It can be seen that k_{L1} was higher than k_{d1}, and k_{L2} is higher than k_{d2}, indicating a higher swelling rate for superabsorbent sponge. These findings suggest that the original hydrogel cross-linking network remained in the superabsorbent sponge, and a porous structure was formed during the freeze-drying. Water can penetrate the network rapidly due to capillary action, and most of the relatively isolated polymer chain segments were disentangled and expended in the water. The carboxyl groups were gradually exposed and combined with water molecules through hydrogen bonding, leading to a high water absorption rate. In contrast, the superabsorbent membrane was non-porous and had a much denser surface structure, which made it difficult for the water to penetrate into the inside of the gel. In addition, superabsorbent membrane polymer chains were further entangled and stacked during the drying process. Therefore, the disentanglement of the polymer chain segments was slower than that of superabsorbent sponge, and less carboxyl groups were exposed during the swelling process, leading to a slower water absorption rate.

Table 1. Swelling Kinetics Parameters of Superabsorbent Membrane

C_{CMC} (wt%)	τ_{d1} (min^{-1})		K_{d1} (min^{-1})		Q_{d1} (%)	
	Pure water	Saline water	Pure water	Saline water	Pure water	Saline water
3.0	11.825	16.622	1.882	0.738	28.07	25.27
3.5	12.289	16.787	1.559	0.697	25.66	22.71
4.0	12.528	17.516	1.146	1.146	22.65	21.03
4.5	12.609	18.047	1.041	1.041	19.69	14.95
5.0	13.017	19.076	0.942	0.942	19.02	13.62
$m_{Al^{3+}}/m_{(CMC+HEC)}$ (%)	τ_{d2} (min^{-1})		K_{d2} (min^{-1})		Q_{d2} (%)	
	Pure water	Saline water	Pure water	Saline water	Pure water	Saline water
0.496	11.868	13.744	1.541	1.005	36.41	24.18
0.744	12.514	14.434	1.309	0.812	31.82	22.94
0.992	13.065	14.717	1.187	0.757	30.57	21.49
1.239	13.360	16.287	0.859	0.532	25.57	13.95
1.488	16.689	16.872	0.281	0.207	9.27	6.82

Note:

a. τ_{d1} and τ_{d2} are the relaxation time for membrane with different amounts of CMC/HEC and aluminium ions.

b. K_{d1} and K_{d2} are the slope of the theoretical curve from time 0 to the time reaching 70% equilibrium swelling ratio.

c. Q_{d1} and Q_{d2} are the equilibrium swelling ratio.

Table 2. Swelling Kinetics Parameters of Superabsorbent Sponge

C_{cmc} (wt%)	τ_{L1} (min^{-1})		K_{L1} (min^{-1})		K'_{L1} (min^{-1})		Q_{L1} (%)	
	Pure water	Saline water	Pure water	Saline water	Pure water	Saline water	Pure water	Saline water
3.0	12.274	3.252	5.201	1.999	23.181	14.401	130.91	46.67
3.5	12.916	3.491	3.538	1.916	22.475	13.465	111.91	44.38
4.0	13.719	4.404	3.301	1.851	22.391	11.692	102.12	42.66
4.5	14.091	4.196	3.196	1.767	17.692	11.885	91.41	41.06
5.0	16.385	4.227	2.455	1.561	17.345	10.975	85.89	39.32
$m_{Al^{3+}}/m_{(CMC+HEC)}$ (%)	τ_{L2} (min^{-1})		K_{L2} (min^{-1})		K'_{L2} (min^{-1})		Q_{L2} (%)	
	Pure water	Saline water	Pure water	Saline water	Pure water	Saline water	Pure water	Saline water
0.496	9.721	3.702	2.355	1.624	27.225	14.232	88.94	45.50
0.744	9.989	3.383	1.756	1.149	25.471	13.941	77.45	39.58
0.992	10.976	4.607	1.693	0.984	19.945	10.875	73.05	33.07
1.239	11.621	6.695	1.384	0.692	10.092	8.075	48.22	25.69
1.488	12.336	7.346	1.114	0.431	4.3515	5.785	21.57	18.34

Note:

a. τ_{L1} and τ_{L2} are the relaxation time for sponge with different amounts of CMC/HEC and aluminium ions.

b. K_{L1} and K_{L2} are the slope of the theoretical curve from time 2 to time 8, and K'$_{L1}$ and K'$_{L2}$ are the slope of the theoretical curve from time 0 to time 2.

c. Q_{L1} and Q_{L2} are the equilibrium swelling ratio for superabsorbent sponge with different amounts of CMC/HEC and aluminium ions.
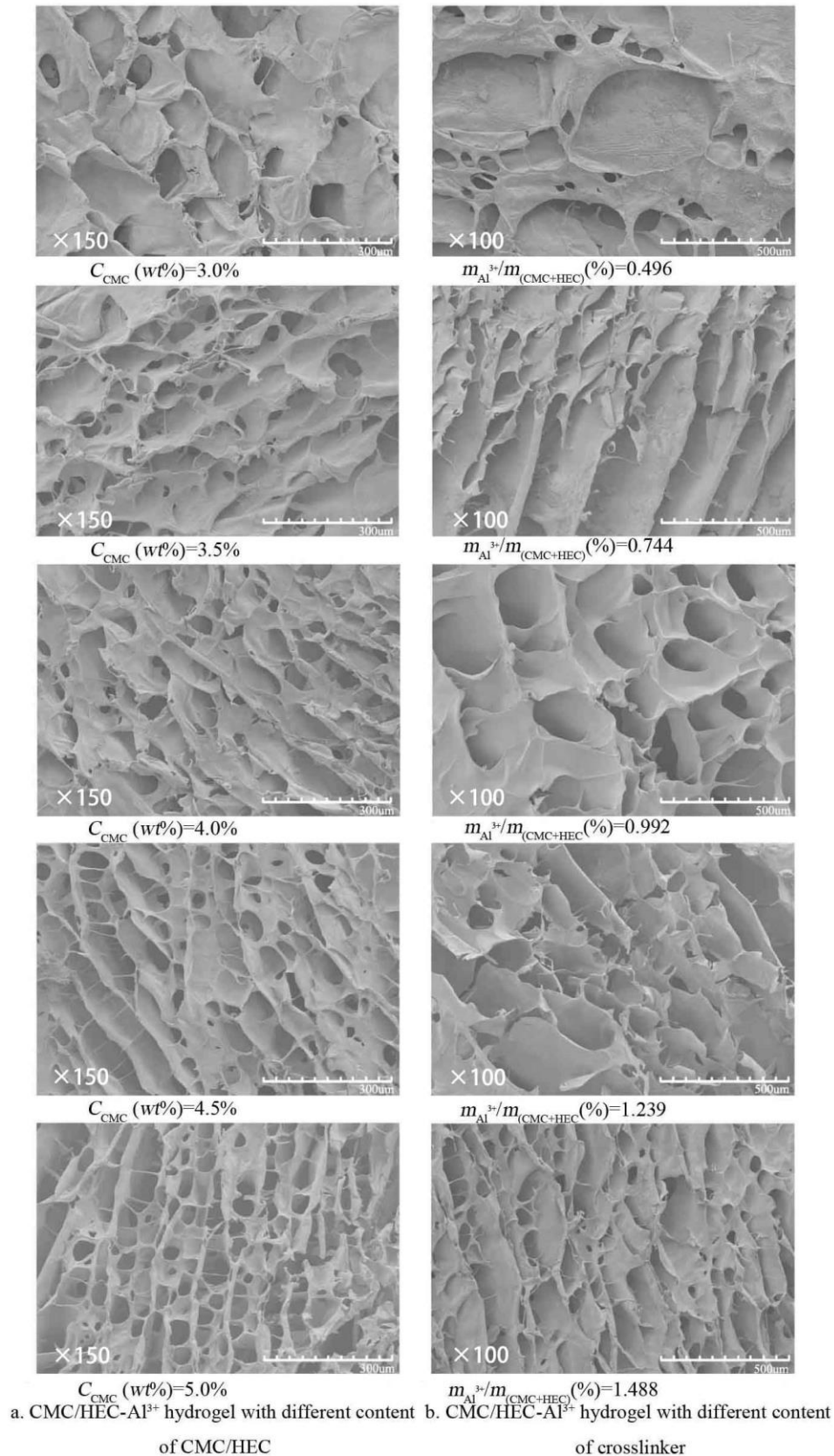
Fig. 5. Effect of CMC/HEC (a) and cross-linker (b) content on the surface morphology of CMC/HEC-Al^{3+} superabsorbent sponge

Figure 5 shows the surface morphologies of water superabsorbent sponges with various CMC/HEC and aluminum ion contents. Well-defined interconnected three-dimensional porous structures were found in all samples. The pores acted as microchannels, which allowed for rapid convection and diffusion of water. The intensities of the pore and microchannel increased with the increase of CMC/HEC and aluminum ion contents. Therefore, the sponge with lower contents of CMC/HEC and aluminum ion showed a larger porous structure, more rapid water diffusion, and thus a higher absorption rate.

The τ values of the superabsorbent sponge and membrane showed opposite changes with the increase of swelling rate, suggesting that the swelling resistance of polymer segments became stronger with the increase of cross-linking density.

The k_{d1}, k_{d2}, k_{L1}, k'_{L1}, k_{L2}, and k'_{L2} values of both superabsorbent membrane and sponge were gradually reduced with an increase of the contents of CMC/HEC and the cross-linking agent, indicating that the entanglement of polymer chain segments and the crosslink density of the dried hydrogels can affect the water absorption rate. In addition, k'_{L1} and k'_{L2} were much higher than k_{L1} and k_{L2} in the first two minutes, due to the rapid water absorption of the porous structure of superabsorbent sponge under capillary action. Thereafter, the swelling rate of the superabsorbent sponge largely depended on the disentanglement rate of the polymer chain segments.

The absorption rates (k) of the superabsorbent sponge and membrane, in both water and saline solutions, became closer following the increase of cross-linking agent content. The k'_{L2} value of the superabsorbent sponge prepared with a high amount of Al^{3+} in saline water was higher than its k'_{L2} value in distilled water. The stretch resistance (τ_{d2}) of the membrane in water gradually approached, and probably even exceeded, that of the membrane in saline, following an increase in Al^{3+} amount. This can be explained by the fact that aluminum ions can increase the cross-linking density of the gel network, but the porous structure of sponge provides more accessible contact sites between NaCl and its cross-linking structure. The electrostatic composite action between Al^{3+} and $-COO^-$ was inhibited by NaCl once the contact occurred, leading to a decreased cross-linking density and an accelerated swelling rate in saline water. The NaCl can also significantly destroy the cross-linking network structure of superabsorbent sponge, and reduces the stretch resistance of the network structure. The sponge with a high cross-linking agent content showed weaker stretching resistances in saline solution.

On the contrary, the τ and k values of both superabsorbent sponge and membrane did not show a significant change with the increase of CMC/HEC content, especially in saline solution. This can be explained by the fact that the increasing CMC/HEC content only caused a relatively increased physical entanglement between the polymer segments. The carboxyl groups involved in the cross-linking reaction remained unchanged. Therefore, cross-linking density caused by combined electrostatic interaction was barely changed. Therefore, the saline solution showed similar effects on the combined electrostatic interactions, and the swelling behavior of the network structures prepared under different CMC/HEC contents.

In all, the CMC/HEC-Al^{3+} hydrogel showed a high swelling rate in the high concentration salt solution. Generally, the water absorption rate of a conventional chemically cross-linked hydrogel containing –COOH would be significantly reduced in high concentration salt solutions due to the osmotic pressure between the inside and outside of the gel network, leading to shrinkage. Therefore, the CMC/HEC-Al^{3+} hydrogel

prepared in the present work could be used as hemostatic medical accessories to rapidly absorb water in the blood, and accelerate blood coagulation.

However, it is well known that solutions of two different polyelectrolytes often will tend to phase-separate (Kovacevic *et al*. 2007). The cationic aluminum species can be expected to interact strongly with the CMC components, basically precipitating that component out of solution – to the extent that the two kinds of polyelectrolytes might initially be at least partly inter-penetrating. On the other hand, the sudden precipitation, resulting from the addition of aluminum sulfate, may "freeze" the system as non-equilibrium trapped states (Trappe *et al*. 2001; Naderi *et al*. 2004). It could be seen from the SEM of the dried hydrogel, at the reaction conditions of the present study, the formation of the hydrogel was homogeneous, and no heterogeneous structures could be observed. So it appears that the formation of the trapped non-equilibrium states is the dominate crosslinking mechanism of the above CMC/HEC-Al^{3+} system. The microgel between the CMC/HEC-Al^{3+} would be formed firstly, then the above microgel would be crosslinked by the Al^{3+}/$Al(OH)^{2+}$ further and the bulk hydrogel can be formed.

Swelling ratio of CMC/HEC-Al^{3+} hydrogel

The swelling ratios of the hydrogels prepared with various amounts of CMC/HEC and Al^{3+} in water were higher than those of the corresponding hydrogels in saline water. This can be explained by the fact that the sodium ions in saline solution reduced the osmotic pressure between the inside and outside of the hydrogels, leading to lower water uptake ratios. In addition, superabsorbent sponge exhibited higher water uptake ratios than the membrane in both water and saline solutions. The reason for this is that the dense surface structure of superabsorbent membrane inhibits the water from entering into the interior of the hydrogel system. In addition, the oven-drying process promoted the shrinkage of the polymer chain, and enhanced hydrogen bonding and physical entanglement between the chain segments, leading to the higher cross-linking density of superabsorbent membrane. According to the classic Flory theory of elastic gel, with the increase of the network density, the chains between crosslinking joints become shorter, and the water absorption ratio decreases.

The CMC/HEC content showed a slight effect on the water uptake ratios of superabsorbent membrane and sponge in both water and saline solution (Tables 1 and 2). As discussed above, the cross-linking density of the hydrogel system was mainly affected by the content of the cross-linking agent. Therefore, changing the CMC/HEC content cannot significantly affect the water uptake ratio of the hydrogel. In contrast, increasing the mass fraction of aluminum in the hydrogel promotes the effects of electrostatic interactions in forming a network, leading to a shorter distances between the polymer chains. Meanwhile, the entanglement and hydrogen bonding between the polymer chains were remarkably enhanced. Consequently, the cross-linking density of the hydrogel was changed, leading to the different absorption ratios of the hydrogels with various Al^{3+} contents. The water uptake ratios of the superabsorbent sponge and membrane decreased more rapidly in water than in saline solution with the increase of CMC/HEC and Al^{3+} content. This can also be attributed to the destroyed combined effects of electrostatic between Al^{3+} and –COO^- in the saline solution.

In full, the water absorption behavior of the hydrogel is affected by the combined effects of electrostatic, chemical cross-linking, and intra- and intermolecular hydrogen bonding. The effects of electrostatic interactions between Al^{3+} and –COO^- were dominant. An increase of the electrostatic effects led to a shorter distance between the polymer

chains, and enhanced the entanglement and hydrogen bonding interactions. On the contrary, physical entanglement and hydrogen bonding between CMC and HEC belong to secondary cross-linking. Their changes were not sufficient to affect the electrostatic effect between Al^{3+} and $-COO^-$.

Thermal Stability of CMC/HEC-Al³⁺ Hydrogel

The thermal stabilities of the superabsorbent membrane and sponge with various CMC/HEC and aluminium ion contents were investigated using TG and DTG analyses. The TG and DTG curves are shown in Fig. 6, and the corresponding thermal decomposition parameters are listed in Table 3. Both superabsorbent sponge and membrane were subjected to two major degradation stages. Dehydration occurred in the temperature range of 30 to 110 °C. The weight loss in the temperature range of 240 to 340 °C could be attributed to the decomposition of cross-linking joints of the network structure, and the destruction of the pyran ring of CMC and HEC. The maximum degradation rate temperature and the temperatures required for 5% and 10% weight loss, gradually increased with the increase of CMC/HEC content.

a. CMC/HEC-Al³⁺ hydrogel with different amount of CMC/HEC

b. CMC/HEC-Al³⁺ hydrogel with different amount of CMC/HEC

c. CMC/HEC-Al³⁺ hydrogel with different amount of crosslinker

d. CMC/HEC-Al³⁺ hydrogel with different amount of crosslinker
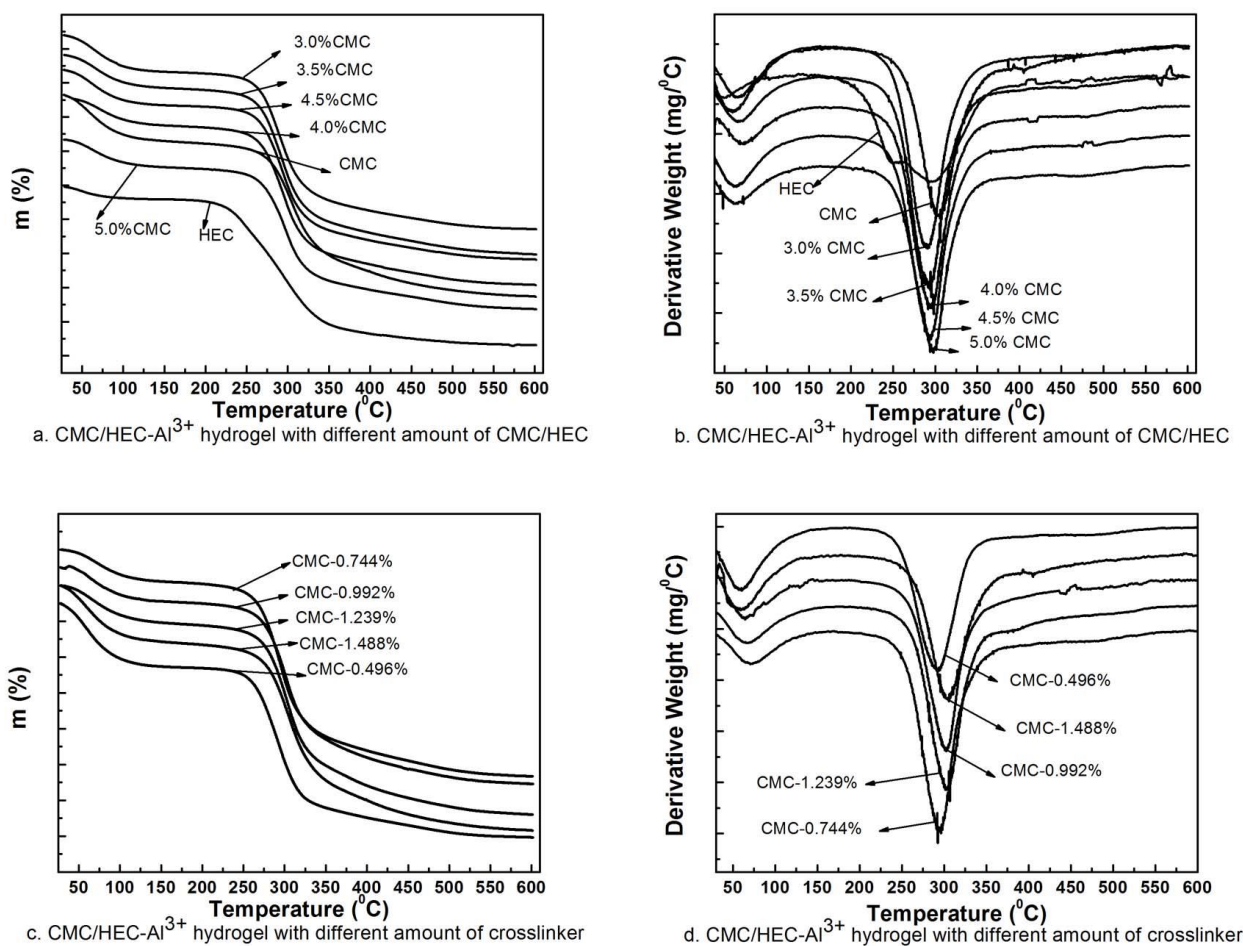
Fig. 6. TG (a, c) and DTG (b, d) curves of the CMC/HEC-Al³⁺ hydrogel with different amounts of CMC/HEC or cross-linker

These specific weight loss temperatures were higher than those of HEC but lower than those of CMC. This can be explained by the fact that the increase of CMC/HEC content leads to a tenser entanglement between the polymer chain segments, more intra- and intermolecular hydrogen bonds between CMC and HEC, and a more stable cross-linking structure. Therefore, the temperature required for the decomposition of the hydrogel is higher than that for the decomposition of HEC. However, the high heat conductive aluminum ions in the composite can accelerate the destruction of the coordinative bond between Al^{3+} and $–COO^-$ at high temperatures. Therefore, the hydrogel exhibited lower thermal decomposition temperatures than CMC.

Table 3. Thermal Analysis Data of CMC, HEC, and Different CMC/HEC-Al^{3+} Hydrogel

Material	Decomposition stage	Temperature(°C)	T_{max} (°C)	Weight loss (%)	Total weight loss (%)	$T_{5\%}$ (°C)	$T_{10\%}$ (°C)
CMC	1	35-109	64	11.09	47.38	278	286
	2	261-316	304	36.29			
HEC	1	30-108	57	7.66	67.82	234	245
	2	205-358	249	60.16			
$m_{Al^{3+}}/m_{(CMC+HEC)}(\%)=$ 0.496	1	32-110	69	15.17	49.72	269	279
	2	251-327	289	34.55			
$m_{Al^{3+}}/m_{(CMC+HEC)}(\%)=$ 0.744	1	35-105	82	7.31	45.37	271	280
	2	249-333	292	38.06			
$m_{Al^{3+}}/m_{(CMC+HEC)}(\%)=$ 0.992	1	36-106	77	8.15	41.46	279	289
	2	257-334	302	33.31			
$m_{Al^{3+}}/m_{(CMC+HEC)}(\%)=$ 1.239	1	39-103	77.46	7.88	41.61	283	292
	2	267-338	305	33.73			
$m_{Al^{3+}}/m_{(CMC+HEC)}(\%)=$ 1.488	1	30-101	70	12.91	45.71	285	295
	2	265-342	308	32.79			
3.0%CMC	1	31-109	75	10.73	47.84	270	279
	2	249-331	285	37.11			
3.5%CMC	1	33-103	77	8.79	47.07	270	279
	2	245-330	290	38.28			
4.0%CMC	1	40-110	82	8.01	47.13	270	280
	2	244-332	292	39.12			
4.5%CMC	1	30-106	73	10.09	46.72	272	281
	2	251-335	294	36.63			
5.0%CMC	1	30-115	74	9.36	46.86	273	283
	2	253-335	297	37.5			

Moreover, the content increase of the cross-linking agent led to an increase of the thermal decomposition temperature for the maximum rate from 293 °C to 308 °C. The temperature for 5% weight loss increased from 269 °C to 285 °C, and that for 10% weight loss increased from 279 °C to 295 °C. The decomposition temperatures of all hydrogels prepared in the present work were higher than the corresponding thermal decomposition temperatures of HEC. However, only the temperatures for the maximum degradation rate, 5% weight loss, and 10% weight loss of the hydrogels with high Al^{3+}

content were higher than those for the corresponding thermal decompositions of CMC. This can be explained by the fact that the cross-linking density of the hydrogel increased with greater cross-linker content. When the aluminum ion content is low, the cross-linked network structure is not completely constructed. The high heat conduction of aluminum ions can destroy some of the coordinative bonds between Al^{3+} and $-COO^-$, and destroy the cross-linked structure, leading to a relatively lower thermal stability of the CMC component in the hydrogel. However, the cross-linked network structure becomes denser and more completely constructed when Al^{3+} contents are higher than a certain value. The distance between the polymer chains becomes shorter, and the entanglement and hydrogen bonding between the CMC and HEC are enhanced. The high heat conduction of aluminum ions only destroyed a small amount of the coordinative bonds between Al^{3+} and $-COO^-$, and a relatively complete cross-linked network structure remained. Therefore, the thermal stability of the hydrogels with higher Al^{3+} contents was higher than that of CMC. The above analyses indicate that the combined electrostatic effect between Al^{3+} and $-COO^-$ are the dominant force, which is consistent with the conclusion from the swelling behavior analysis.

CONCLUSIONS

1. A superabsorbent hydrogel was successfully prepared using the cross-linking of CMC/HEC with aluminum ions. The mass ratio of aluminum cationic species to CMC/HEC and the CMC/HEC content in a hydrogel could significantly affect its cross-linking structure and properties.

2. Swelling rate analyses of CMC/HEC-Al^{3+} hydrogel indicated that the electrostatic composite action between Al^{3+} and $-COO^-$ was inhibited by NaCl once the contact occurs, leading to a decreased cross-linking density and an accelerated swelling rate in saline water. On the contrary, the τ and k values of both superabsorbent sponge and membrane did not show a significant change with the increase of CMC/HEC content, especially in saline solution. This could be explained by the fact that increasing the CMC/HEC content only caused a relatively increased physical entanglement between the polymer segments.

3. Swelling ratio analyses of CMC/HEC-Al^{3+} hydrogel showed that an increase of electrostatic effect leads to a shorter distance between the polymer chains and enhances the entanglement and hydrogen bonding interactions. On the contrary, physical entanglement and hydrogen bonding between CMC and HEC belonged to secondary cross-linking. Their changes were not sufficient to affect the electrostatic effect between Al^{3+} and $-COO^-$.

4. The structure of the CMC/HEC-Al^{3+} hydrogels was determined using FTIR and rheological analyses. The results indicated that bidentate ligand reactions occurred between the aluminum ion and the carboxyl group of CMC.

5. TG and DTG analysis showed that the high heat conduction of aluminum ions and the contents of CMC/HEC and Al^{3+} had a big influence on the thermal stability of the hydrogel. Meanwhile, electrostatic effect, physical entanglement, and intra- and intermolecular hydrogen bonds contributed to the network building of the cross-linked hydrogel with the electrostatic effect acting as the dominant force.

ACKNOWLEDGMENTS

REFERENCES CITED

Barbucci, R., Magnani, A., and Consumi, M. (2000). "Swelling behavior of carboxymethylcellulose hydrogels in relation to cross-linking, pH, and charge density," *Macromolecules* 33(20), 7475-7480. DOI: 10.1021/ma0007029

Bi, S., Wang, C., Cao, Q., and Zhang, C. (2004). "Studies on the mechanism of hydrolysis and polymerization of aluminum salts in aqueous solution: Correlations between the "Core-links" model and "Cage-like" Keggin-Al_{13} model," *Coordination Chemistry Reviews* 248, 441-455. DOI: 10.1016/j.ccr.2003.11.001

Cai, J., and Zhang, L. (2006). "Unique gelation behavior of cellulose in NaOH/urea aqueous solution," *Biomacromolecules* 7(1), 183-189. DOI: 10.1021/bm0505585

Chang, C., Duan, B., Cai, J., and Zhang, L. (2010). "Superabsorbent hydrogels based on cellulose for smart swelling and controllable delivery," *European Polymer Journal* 46(1), 92-100. DOI: 10.1016/j.eurpolymj.2009.04.033

Chen, Y., and Tan, H. (2006). "Crosslinked carboxymethylchitosan-g-poly(acrylic acid) copolymer as a novel superabsorbent polymer," *Carbohydrate Research* 341(7), 887-896. DOI: 10.1016/j.carres.2006.01.027

Chen, Y., Liu, Y., Tan, H., and Jiang, J. (2009). "Synthesis and characterization of a novel superabsorbent polymer of N, O-carboxymethyl chitosan graft copolymerized with vinyl monomers," *Carbohydrate Polymers* 75(2), 287–292. DOI: 10.1016/j.carbpol.2008.07.022

Chen, Y., Liu, Y., Tang, H., and Tan, H. (2010). "Study of carboxymethyl chitosan based polyampholyte superabsorbent polymer. I. Optimization of synthesis conditions and pH sensitive property study of carboxymethyl chitosan-g-poly (acrylic acid-co-dimethyldiallylammonium chloride) superabsorbent polymer," *Carbohydrate Polymers* 81(2), 365-371. DOI: 10.1016/j.carbpol.2010.02.007

Chen, Y., Liang, Y. Are, Y., Zhang, Y., Ding, Y., Guo, Y., Ye, Y., and Tan, H. (2012). "Structure and drug release of superabsorbent sponge prepared by polyelectrolyte complexation and freezing-induced phase separation," *Journal of Applied Polymer Science* 126(4), 1307-1315. DOI: 10.1002/app.36937

Coviello, T., Matricardi, P., Balena, A., Chiapperino, B., and Alhaique, F. (2010). "Hydrogels from scleroglucan and ionic crosslinkers: Characterization and drug delivery," *Journal of Applied Polymer Science* 115(6), 3610-3622. DOI: 10.1002/app.31375

Gao, X., Cao, Y., Song, X., Zhang, Z., Zhuang, X., He, C., and Chen, X. (2014). "Biodegradable, pH-responsive carboxymethyl cellulose/poly(acrylic acid) hydrogels for oral insulin delivery," *Macromolecular Bioscience* 14(4), 565-575. DOI: 10.1002/mabi.201300384

Hubbe, M. A., Ayoub, A., Daystar, J. S., Venditti, R. A, and Pawlak, J. J. (2013). "Enhanced absorbent products incorporating cellulose and its derivatives: A review," *BioResources* 8(4), 6556-6629.

Ibrahim, S. M., Abou El Fadl, F. I., and El-Naggar, A. A. (2014). "Preparation and characterization of crosslinked alginate-CMC beads for controlled release of nitrate salt," *Journal of Radioanalytical and Nuclear Chemistry* 299(3), 1531-1537. DOI: 10.1007/s10967-013-2820-4

Kono, H. (2014). "Characterization and properties of carboxymethyl cellulose hydrogels crosslinked by polyethylene glycol," *Carbohydrate Polymers* 106, 84-93. DOI: 10.1016/j.carbpol.2014.02.020

Kono, H., and Fujita, S. (2012). "Biodegradable superabsorbent hydrogels derived from cellulose by esterification crosslinking with 1,2,3,4-butanetetracarboxylic dian-hydride," *Carbohydrate Polymers* 87(4), 2582–2588. DOI: 10.1016/j.carbpol.2011.11.045

Kovacevic, D., Borkovic, S., and Pozar, J. (2007). "The influence of ionic strength, electrolyte type and preparation procedure on formation of weak polyelectrolyte complexes," *Colloids and Surfaces A-Physicochemical and Engineering Aspects* 302(1-3), 107-112. DOI: 10.1016/j.colsurfa.2007.02.007

Laçin, N. T. (2014). "Development of biodegradable antibacterial cellulose based hydrogel membranes for wound healing," *International Journal of Biological Macromolecules* 67, 22-27. DOI: 10.1016/j.ijbiomac.2014.03.003

Liu, Z., Miao, Y., Wang, Z., and Yin, G. (2009). "Synthesis and characterization of a novel super-absorbent based on chemically modified pulverized wheat straw and acrylic acid," *Carbohydrate Polymers* 77(1), 131-135. DOI: 10.1016/j.carbpol.2008.12.019

Naderi, A., Claesson, P. M., Bergstrom, M., and Dedinaite, A. (2004). "Trapped non-equilibrium states in aqueous solutions of oppositely charged polyelectrolytes and surfactants: effects of mixing protocol and salt concentration," *Colloids and Surfaces A-Physicochemical and Engineering Aspects* 253(1-3), 83-93. DOI: 10.1016/j.colsurfa.2004.10.123

Nakamoto, K. (2008). "Infrared and raman spectra of inorganic and coordination compounds: Part B: Applications in coordination, organometallic, and bioinorganic chemistry," in: *Applications in Coordination Chemistry*, K. Nakamoto. (ed.), John Wiley & Sons, Inc., Hoboken, New Jersey. DOI: 10.1002/9780470405888.ch1

Nerurkar, N. L., Elliott, D. M., and Mauck, R. L. (2010). "Mechanical design criteria for intervertebral disc tissue engineering," *Journal of Biomechanics* 43(6), 1017-1030. DOI: 10.1016/j.jbiomech.2009.12.001

Omidian, H., Park, K., Kandalam, U., and Rocca, J. G. (2010). "Swelling and mechanical properties of modified HEMA-based superporous hydrogels," *Journal of Bioactive and Compatible Polymers* 25(5), 483-497. DOI: 10.1177/0883911510375175

Saha, N., Saarai, A., Roy, N., Kitano, T., and Saha, P. (2011). "Polymeric biomaterial based hydrogels for biomedical applications," *Journal of Biomaterials and Nanobiotechnology* 2(1), 85–90. DOI: 10.4236/jbnb.2011.21011

Schrecker, S.T., and Gostomski, P. A. (2005). "Determining the water holding capacity of microbial cellulose," *Biotechnology Letters* 27(19), 1435-1438. DOI: 10.1007/s10529-005-1465-y

Seki, Y., Altinisik, A., Demircioglu, B., and Tetik, C. (2014). "Carboxymethylcellulose (CMC)-hydroxyethylcellulose (HEC) based hydrogels: synthesis and characterization," *Cellulose* 21(3), 1689-1698. DOI: 10.1007/s10570-014-0204-8

Tang, H., Chen, H., Duan, B., Lu, A., and Zhang, L. (2014). "Swelling behaviors of superabsorbent chitin/ carboxymethylcellulose hydrogels," *Journal of Materials Science* 49(5), 2235-2242. DOI: 10.1007/s10853-013-7918-0

Trappe, V., Prasad, V., Cipelletti, L., Segre, P. N., and Weitz, D.A. (2001). "Jamming phase diagram for attractive particles," *Nature* 411(6839), 772-775. DOI: 10.1038/35081021

Weng, L., Zhang, L., Ruan, D., Shi, L., and Xu, J. (2004). "Thermal gelation of cellulose in a NaOH/thiourea aqueous solution," *Langmuir* 20(6), 2086-2093. DOI: 10.1021/la035995o

Yang, X., and Zhu, W. (2007). "Viscosity properties of sodium carboxymethylcellulose solutions," *Cellulose* 14(5), 409-417. DOI: 10.1007/s10570-007-9137-9